C. H. Wang and M. W. Brown†*

Multiaxial Random Load Fatigue: Life Prediction Techniques and Experiments

REFERENCE Wang, C. H. and Brown, M. W., **Multiaxial random load fatigue: life prediction techniques and experiments**, *Multiaxial Fatigue and Design*, ESIS 21 (Edited by A. Pineau, G. Cailletaud, and T. C. Lindley) 1996, Mechanical Engineering Publications, London, pp. 513–527.

ABSTRACT Fatigue under multiaxial random loading is a large and intractable topic, on which there has been little research effort. Few life prediction methodologies have so far been proposed in the literature for evaluation of fatigue damage under complex loading histories. An extensive biaxial random load test programme was conducted at room temperature to study fatigue damage behaviour under multiaxial loading and to provide a basis for evaluation of two methods. Computer codes were developed that implemented these methods, and predictions are compared with the test results. In theory these two methods can be considered as bounding solutions for fatigue damage accumulation, providing acceptable predictions of endurance for En15R steel.

1 Introduction

The evaluation of fatigue damage under complex states of stress and strain is attracting increasing attention as requirements for engineering design of structures under complex service loading become more stringent. With the advance of computer technology, an indispensable design tool, it is now not only desirable but also possible to develop viable fatigue life prediction methods capable of dealing with complicated service loading. The type of loading encountered in many components and structures during their service life may be random and/or nonproportional; examples are pressure vessels, gas turbines, automobile crankshafts and nuclear reactors. The inherent complexities of stress–strain state and loading history render impossible the use of traditional life prediction methods, such as those developed for uniaxial variable amplitude loading, since there is more than one variable to consider with respect to time in the case of multiaxial random loading.

For a triaxial stress state, up to six independent stress components may vary with time. Both the directions of principal stresses and the ratios between them may fluctuate. Counting methods and stochastic processes have usually been applied to uniaxial loading, where there is a single variable to consider with respect to time. On the basis that a closed hysteresis loop defines a cycle, several

*School of Engineering and Technology, Deakin University, Geelong, VIC 2317, Australia (presently at: Aeronautical and Maritime Research Laboratory, Department of Defence, 506 Lorimer Street, VIC 3207, Australia).
†SIRIUS, The University of Sheffield, Mappin Street, Sheffield, S1 3JD, UK.

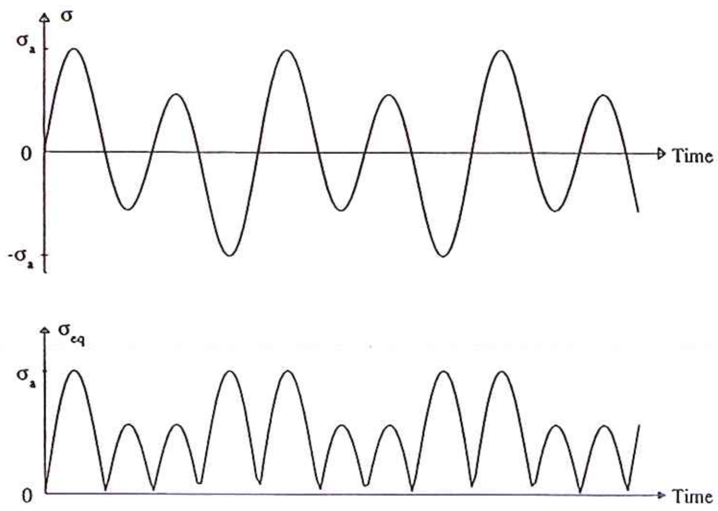

Fig 1 Illustration of problems with the use of cycle counting method on equivalent strain history.

cycle counting methods have been proposed over the last two decades, e.g. Rainflow (1) and range pair (2) methods. These two algorithms have been widely accepted as the best methods for uniaxial random fatigue, being able to provide good correlation with experimental results (3–5). However, there has been comparatively little effort towards the development of a multiaxial cycle counting method. Despite extensive studies (6) and many damage criteria for constant amplitude multiaxial fatigue, these methods are virtually unusable for in-service loading without a suitable cycle counting procedure. Hence the development of life prediction techniques of value to industry for complex service loading has been seriously hindered.

The success of both uniaxial cycle counting and equivalent strain methods in assimilating strains for constant amplitude multiaxial loading into a scalar quantity suggests a viable combination of the two methods. Further study reveals that this would result in erroneous stress or strain range identification and wrong cycle counts. This is because equivalent strain and stress are surds which are always positive. This is best appreciated with reference to Fig. 1, which shows a case of uniaxial variable amplitude loading, demonstrating that as little as half of the actual range may be counted, as the negative half cycles are folded over.

Due to the lack of an appropriate multiaxial cycle counting method, Bannantine and Socie (7,8) proposed a life prediction method based on critical plane concepts (9), in which the unknown damage plane needs to be identified, since the plane that experiences maximum damage governs the lifetime. Since

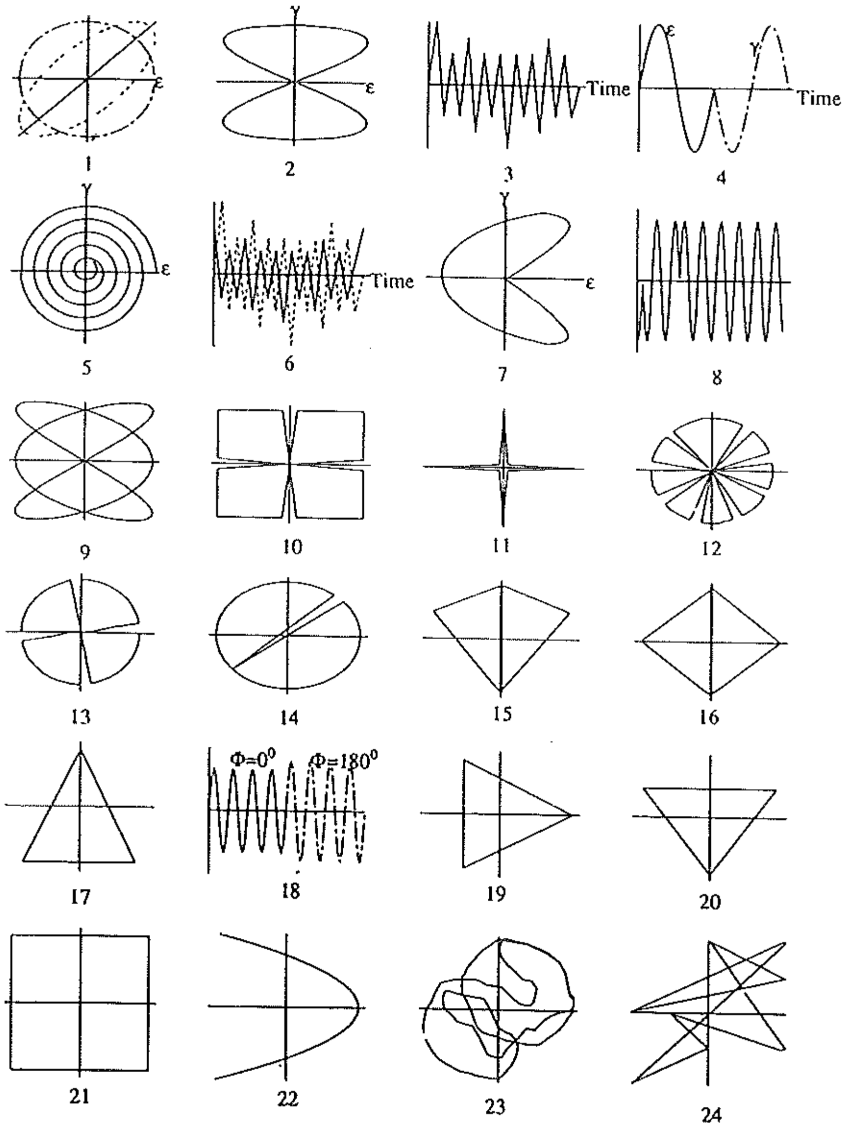

Fig 2 Examples of loading paths, plotted as γ versus ε, or strain versus time.

either the tensile strain normal to, or the shear strain across, a plane is considered, conventional cycle counting methods are applicable. The procedure is a general one which can analyse each loading path shown in Fig. 2 for combined torsional and axial loading.

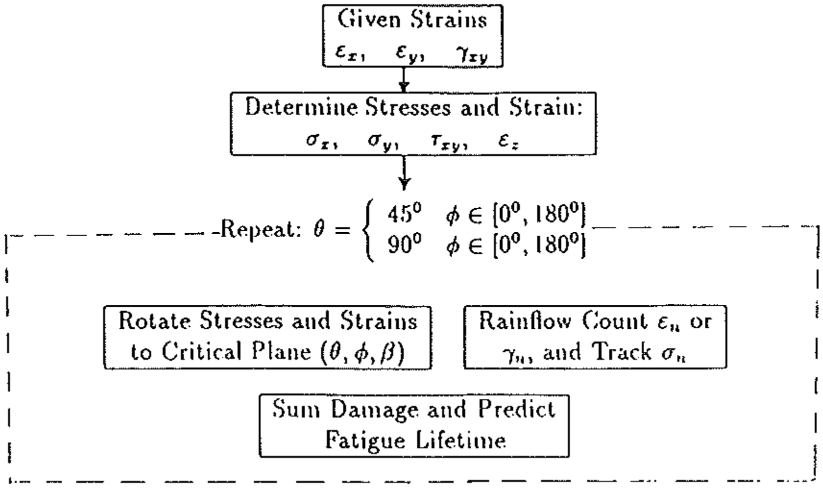

(a) Bannantine and Socie's method.

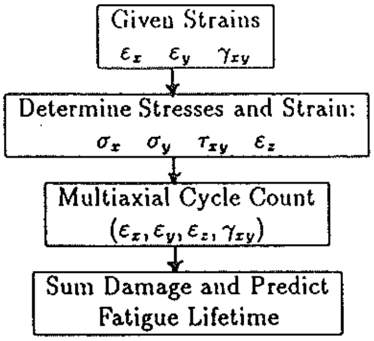

(b) Wang and Brown's method

Fig 3 Flow charts for (a) Bannantine and Socie's method, and (b) Wang and Brown's method.

Wang and Brown (**10**, **11**) recently proposed a cycle counting method on the basis of hysteresis hardening behaviour under nonproportional variable amplitude loading. Relative stresses and strains were introduced, such that a turning point was defined when the equivalent relative strain attained its peak value. Fatigue damage can then be evaluated using a multiaxial parameter, and the overall fatigue damage due to a loading block is added up using Miner's (**12**) linear rule. The following section presents a brief review of these two methods, whose predictions of fatigue endurance will be compared with experimental results.

2 Review of Life Prediction Methods

2.1 *Bannantine and Socie's method*

Bannantine and Socie (7, 8) suggested that fatigue damage events occur on an arbitrary plane, identified by Rainflow counting the strain history acting on that plane. For each plane being considered, strains have to be projected onto it, then either the normal strain or the shear strain is cycle counted using the traditional Rainflow method. The total damage due to a block is summed using Miner's rule. Finally the failure plane is taken to be that plane which experiences the maximum damage. As an example, Fig. 3(a) shows a flow chart for a computer program to solve a surface cracking problem, where cycle counting and damage evaluation modules have to be repeated until all possible planes have been scanned through. Information regarding the dominant fatigue failure modes should be known beforehand in order to select the correct fatigue damage model, either tensile (mode I) or shear (mode III) cracking.

For a tensile crack dominated material, the following damage parameter is used

$$\frac{\Delta\varepsilon_1}{2}\,\sigma_{max} = \frac{\sigma_f'^2}{E}\,(2N_f)^{2b} + \sigma_f'\varepsilon_f'(2N_f)^{b+c}$$

where $\Delta\varepsilon_1/2$ is the maximum principal strain amplitude and σ_{max} is the maximum normal stress on the maximum principal strain plane. The involvement of the maximum stress normal to the plane means that it has to be tracked during cycle counting and its peak value during a given strain reversal determined. Conversely, for a shear crack dominated material, a different parameter is used

$$\frac{\Delta\gamma_{max}}{2}\left(1 + \frac{\sigma_n}{\sigma_y}\right) = \frac{\tau_f'}{G}\,(2N_f)^{b} + \gamma_f'(2N_f)^{c}$$

where $\Delta\gamma_{max}/2$ represents maximum shear strain amplitude and σ_n is the maximum normal stress on the γ_{max} plane. Values of the material constants in these equations are given in Table 1. Fatigue life, N_f, is then determined using the damage calculations on this plane. Attention is needed in choosing σ_y, since a small value would mean that the damage plane in torsion identified by this method would differ from the maximum shear plane, which has been confirmed by experiments to be the plane on which cracks grow. However the actual material yield stress has been used here, whereas the torsional fatigue ductility coefficient γ_f' and fatigue strength coefficient τ_f' have been fitted to fully reversed torsional fatigue data using the above shear crack parameter, which incorporates the mean stress correction.

Table 1 Material parameters for En15R steel

E (GPa)	ν	σ_f' (MPa)	ε_f'	b	c	S
205	0.28	1114	0.259	−0.097	−0.515	1.38

σ_y (MPa)	γ_f'	τ_f' (MPa)
623	0.664	989.0

Consider the general case of random loading, and denote the normal to the damage plane under consideration as (cos θ, cos ψ, cos α), where

$$\cos \alpha = \sqrt{1 - \cos^2 \theta - \cos^2 \psi}$$

Here the same notation is adopted as that used in (**8**). The search procedure has to be carried out for both angles θ (inclination of plane from surface) and ψ (orientation of plane on surface) to scan through 0 to π, demanding a great deal of calculation when a small angle increment is used. Since fatigue cracks often occur on the surface of a component where three surface stresses are zero, only a plane stress state has to be considered. This means that there are only three in-plane stress and strain components and a strain component normal to the surface. The number of planes that have to be searched can be reduced (**8**) by considering only two cases, Case A and Case B (**9**), i.e. $\theta = \pi/4$ and $\pi/2$ with ψ ranging from 0 to π.

2.2 *Wang and Brown's counting method*

Since plastic deformation is the driving force for fatigue damage, hysteresis hardening and history (described by the memory effect) under multiaxial random loading ought to provide a rational basis for a cycle counting method, similar to the uniaxial case. The most significant turning point is associated with the highest plastic strain in a block, and can be identified by the greatest value of equivalent strain (or stress), such as point A in Fig. 4. Starting from point A, a graph is prepared for a complete loading block of relative equivalent strain with respect to A, where relative strain $\varepsilon_{ij}^* = \varepsilon_{ij} - \varepsilon_{ij}^A$ represents strain change since time A, and equivalent strain is on a von Mises basis. Figure 4 shows an example for loading path No. 20 (Fig. 2) under combined axial and torsional strain. Using the relative strain, a reversal can be defined starting from A, up to the maximum value, i.e. AB and CD comprise one reversal where the relative strain increases steadily from A to D. (This procedure is similar to the Rainflow counting method.) Starting with the next turning point B, relative strain is replotted with respect to that turning point for the subsequent continuous fragment of strain history (B to C), yielding a single reversal EF shown in

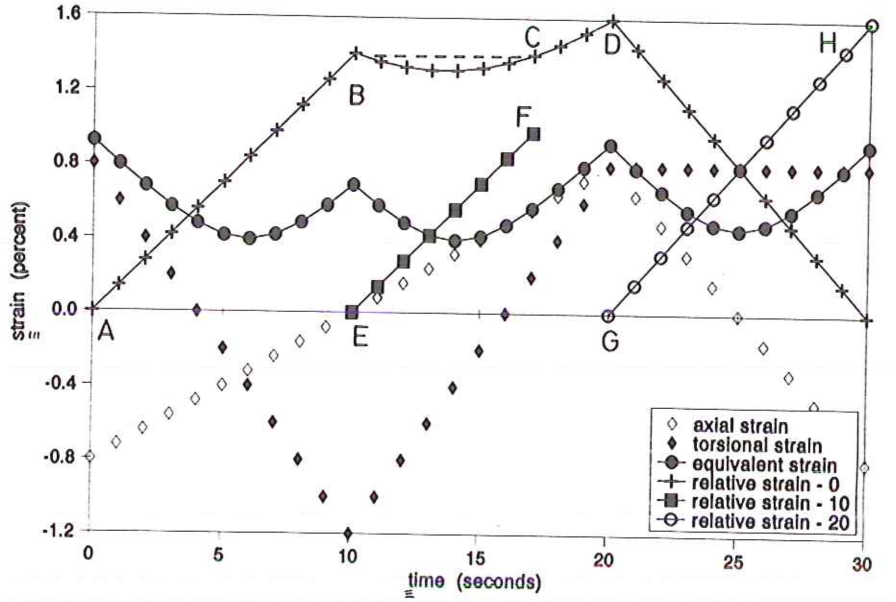

Fig 4 Wang's cycle counting procedure for loading path No. 20.

Fig. 4. This final step is then repeated for each turning point in chronological order until all reversals have been counted for the loading block (GH is the last reversal in Fig. 4), and every fragment of strain history has been counted.

An essential feature of this counting method is its independence from fatigue damage parameters or fatigue cracking behaviour, being based on hysteresis deformation behaviour. This means that its application is independent of material properties or temperature, and it can be integrated with various multiaxial fatigue damage models. Since the counted reversals are in general of nonproportional nature, a fatigue damage parameter capable of accounting for nonproportional straining effects is required. To this end, we adopt the path-independent damage parameter proposed by Wang and Brown (13), which has been demonstrated to provide good correlation for several materials under proportional and nonproportional loading

$$\hat{\varepsilon} \equiv \frac{\gamma_{\max} + S\delta\varepsilon_n}{1 + \nu' + S(1 - \nu')} = \frac{\sigma_f'}{E}(2N_f)^b + \varepsilon_f'(2N_f)^c$$

where $\gamma_{\max}$ is the maximum shear strain amplitude for a given reversal (proportional and nonproportional), and $\delta\varepsilon_n$ is the normal strain excursion between two turning points of the maximum shear strain (that is the range of normal strain experienced on the maximum shear plane during the time between the start and end of the reversal). Parameter S is a material constant representing sensitivity to crack growth under the normal strain on maximum shear plane, and ν' is the effective Poisson's ratio. The right-hand side of the equation is the same as the uniaxial strain life equation; hence the four material constants could be generated from uniaxial tests alone, leaving only S to be determined from a multiaxial test. The total damage induced by a loading block is the summation of damage contributions for each reversal. A flow chart of the algorithm is presented in Fig. 3(b).

3 Experiments and Results

An extensive biaxial test programme was conducted on En15R steel, which had the following chemical composition (% wt.): 0.39C, 0.25Si, 1.66Mn, 0.018P, 0.004S, and remainder ferrite. Test conditions covered proportional and nonproportional loading with constant or variable amplitudes, on tubular specimens with inner and outer radii of 8 and 11 mm. Detailed information on the cyclic deformation behaviour and associated material parameters can be found in (14). With the aid of a computer system for control and data acquisition, tests were conducted at room temperature using a strain controlled tension–torsion rig. Figure 2 shows the types of loading path examined, and Table 2 shows an example of the test history for a specimen subjected to several loading blocks. Both axial and shear strains were controlled to follow the imposed loading paths as shown in Fig. 2, whereas the axial and shear feedback strains were recorded to provide the input to fatigue life prediction modules. Fatigue life was defined as the number of blocks applied when a 5% drop in loading range occurred, which normally corresponded to the presence of surface cracks longer than 4 mm. Failure cracks were observed to be of tensile or shear mode, depending upon biaxiality, phase angle, and strain level.

Table 2 Test history of specimen 13

ε_a (%)	γ_a (%)	ϕ (deg)	*Path P* (see Fig. 2)	*Number of blocks* n
0.80	2.01	0	4	31
0.81	1.36	90	6	3
0.00	1.31	0	1	21
0.96	0.51	90	1	21
0.80	2.02	0	4	15
0.80	1.66	0	4	192

Baseline data for the Basquin and Coffin–Manson endurance equations (E, ν, σ_f', ε_f', b, c) were determined from experimental results under uniaxial constant amplitude loading, with the parameter S being identified from a set of torsional test data. These values, listed in Table 1, were used in both life prediction procedures, whereas for Bannantine and Socie's method two additional material constants for shear cracking had to be determined.

Three proportional variable amplitude loading tests were conducted to provide a benchmark for validation of the two damage evaluation methods; both methods were expected to give approximately the same predictions. The loading history consisted of a repeating block with the axial and shear strain being proportional, but with variable amplitude. The load drop at failure was defined from the maximum stress range in a block. Using the same variable amplitude sequence but with a time offset between the two signals, four nonproportional variable amplitude tests were performed. The loading was both nonproportional and variable amplitude, an example is path No. 24 shown in Fig. 2. In addition, one test was conducted using a loading sequence measured from an automotive vehicle suspension, which had 440 turning points. The rest of the experiments were under truly multiaxial random loading: each specimen was subjected to a number of different loading blocks (proportional or nonproportional variable amplitude), without restriction to the sequence or repetition of blocks. For example, test 13 experienced six blocks of four different loading sequences, as shown in Table 2, providing six stress–strain data files. A detailed account of all tests can be found in **(15)**.

4 Discussion

4.1 *Theoretical considerations*

Since the Bannantine and Socie method assumes that fatigue cracks only propagate in a coplanar manner throughout lifetime and only the strain acting on this plane is effective, no account is taken of crack branching and consequent multistage propagation processes. The method is probably more suitable for loading histories of single repeating blocks of relatively short length. In this case, crack advance per block would be very small with lifetimes of a large number of blocks; therefore cracks would grow essentially in only one direction. By contrast, for those cases where the loading history is random (narrow band) or endurance is a few long blocks, cracks may change to faster growth paths, so Bannantine and Socie's method would underestimate fatigue damage. Wang's method goes to the other extreme, allowing the critical plane to change in every reversal. Several other factors have also been neglected in both procedures, such as the T-stress effect on crack growth **(16, 17)**, mixed mode cracking **(18)**, change in crack morphology due to changes in loading system **(19)**, etc., causing nonconservative predictions.

It is noted that Palmgren–Miner's cumulative damage law is used in both life prediction methods. Despite its shortcomings of failing to describe some load sequence effects, Miner's linear rule is the simplest and most effective method for estimating damage accumulation **(20, 21)**. This can be attributed to the fact that it is firmly based on the integration of a stage II crack growth law, which also largely accounts for its deficiency as stage I cracking is ignored. A

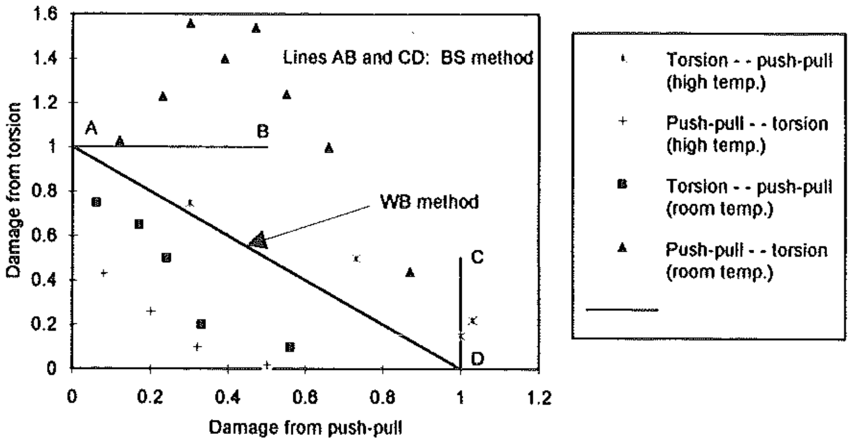

Fig 5 Comparison of Bannantine and Socie's with Wang and Brown's methods for sequential loading, for stainless steel at high temperature (23) and medium carbon steel at room temperature (20).

two-stage crack growth model may offer a better simulation of damage, although more information on crack growth behaviour is needed. This is further complicated in the case of multiaxial loading where a change in loading mode, or the rotation of principal axes, may alter fatigue endurance (**22**). Overall, Miner's rule provides a simple yet satisfactory correlation to many loading histories.

When the loading sequence effect is ignored and Miner's linear rule is invoked to sum damage for each counted reversal, Wang and Brown's method should provide a lower bound solution to fatigue damage, and Bannantine and Socie's method an upper bound. This is because Wang and Brown take the damage of each reversal to be the maximum possible value, irrespective of crack orientation. To elucidate this point, let us consider sequential loading, in which torsional cycling is followed by push-pull loading, or vice versa. Ibrahim (**20**) and Zhang (**21**) reported that at room temperature the damage summation may approach 1.8 for torsion after push-pull, whereas the damage can be as low as 0.3 for push-pull after torsion. This was ascribed to the change of principal stress direction in relation to crack orientation (**22**). However, Weiss and Pineau (**23**) reported that, at elevated temperature, the damage summations in both cases were below unity, and moreover, sequential torsion push-pull was less detrimental than sequential push-pull torsion loading, due to different cracking behaviour.

Figure 5 shows damage summation for sequential tension torsion loading. According to Bannantine and Socie, the failure crack is either tensile or shear; that means the lifetime is determined by either the tensile strain (stress) or the shear strain (stress) across the critical plane. As a result, for tensile failure the torsion cycling would have no effect, and vice versa. This corresponds to the

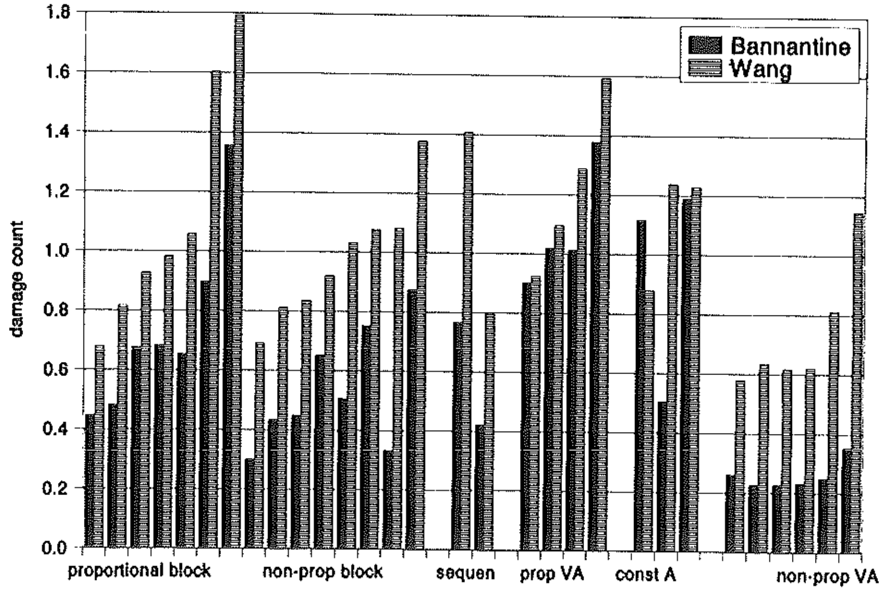

Fig 6 Fatigue damage summation for all tests, comparing Bannantine and Socie's method with Wang and Brown's method.

two separate curves AB and CD in Fig. 5. For the same loading history, Wang and Brown's method would predict damage curve AD. It is noted that neither method accounts for the loading sequence, *viz* the same results are predicted for tension followed by torsion, or torsion followed by tension. Included in the figure are experimental results obtained by Ibrahim (**20**) at room temperature and by Weiss and Pineau (**23**) at elevated temperature (600°C), confirming that both methods fail to represent correctly mixed-mode cracking and changes in crack path.

4.2 *Comparison between results and predictions*

Computer codes implementing the two methodologies have been developed, and the damage results are compared in Fig. 6 where a value of unity implies a perfect prediction. For given strain histories, the corresponding stress histories were computed by means of a plasticity model (**14**) suitable for multiaxial random loading. For Bannantine and Socie's method, calculations of fatigue damage were performed on a set of planes in increments of 2 degrees (for angle ϕ). For combined tension–torsion tests, the angle θ was taken to be $\pi/2$, so only Case A was considered. For each loading block, damage due to tensile cracking and shear cracking were evaluated on 90 planes, so that a total of 180 cycle counting and damage evaluation passes were involved.

By contrast, Wang and Brown's method required only one cycle counting pass for each loading block. Since most tests involved more than one loading block, Wang and Brown summed damage over each block to give the total damage. Bannantine and Socie's method, however, had to compare the damage summation associated with the 180 candidate planes for all the loading blocks, and the fracture plane was then defined as that experiencing the maximum damage.

4.3 *Proportional and nonproportional variable amplitude loading*

The good correlation of the predictions with experimental results under proportional variable amplitude loading, as shown in Table 3, revealed that both methods are accurate in counting cycles and estimating fatigue damage. The experimental endurances are plotted in Fig. 7 together with predicted endurances from the two methods. The minor discrepancy between the predictions of the two methods is due to the differences in fatigue endurance equations; Wang and Brown's method used a multiaxial criterion with $S = 1.38$, whereas Bannantine and Socie adopted the maximum tensile strain criterion ($S = 1.0$). Reasons for the good correlation between experimental and predicted lifetimes include: cycle counting being analogous to uniaxial random loading, co-planar crack growth, and no nonproportional straining effect. The results also demonstrate that the computer codes developed here are consistent.

Table 3 Comparison between experimental and predicted lifetimes

Test No.	*Loading conditions*	*Experimental life (blocks)*	*Predicted life (blocks)* Bannantine	Wang
7	Prop. var. ampl.	366	411	398
20	Prop. var. ampl.	1854	1910	1464
22	Prop. var. ampl.	340	342	314
23	Prop. var. ampl.	1088	865	689
15	Nonprop. var. ampl.	1780	8145	2960
18	Nonprop. var. ampl.	957	3881	1709
27	Nonprop. var. ampl.	2348	10779	3949
28	Nonprop. var. ampl.	960	4272	1468
29	Nonprop. var. ampl.	2189	9415	2846
30	Nonprop. var. ampl.	141	379	93

In contrast to this close correlation, predicted endurances by means of Bannantine and Socie's method are between four and five times higher than experimental results, for nonproportional histories. This is in agreement with the work by Bannantine and Socie (7), where the ratio between predicted and experimental endurances lay between three and four. By contrast, Wang and Brown's method offers improved predictions, with the ratios between predicted and measured endurances lying between 0.6 to 1.6 (Fig. 7).

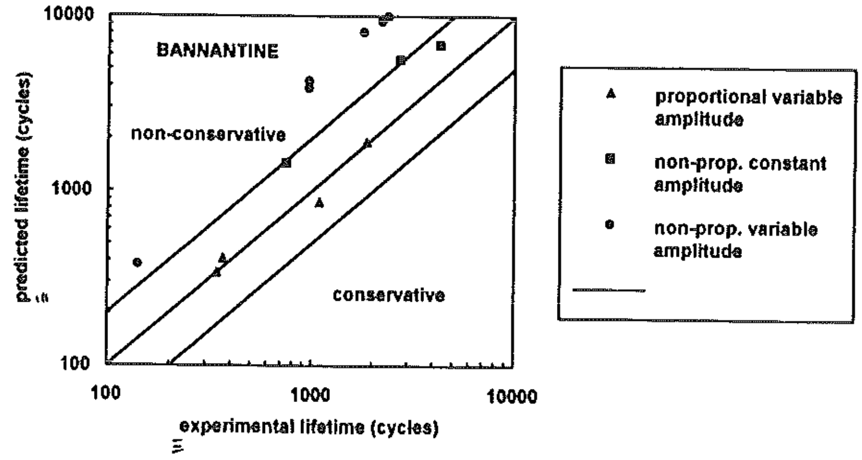

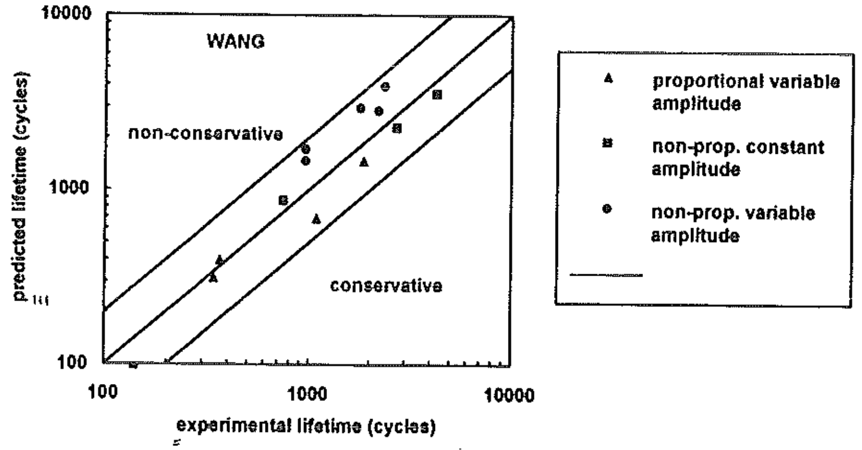

Fig 7 Measured and predicted lifetimes under variable amplitude loading: (a) Bannantine and Socie's method; (b) Wang and Brown's method.

4.4 *Multiaxial random loading*

Since some tests were dominated by proportional loading blocks, predicted damage summation exhibited a mixed picture. Results are plotted in Fig. 6, confirming that Bannantine and Socie's method underestimated damage accumulation for all tests except proportional variable amplitude loading. It may be observed that the damage summations of Bannantine and Socie were consistently smaller than those of Wang and Brown for the 30 tests analysed. Moreover, for the latter case, the average damage value predicted was unity, suggesting that Wang and Brown's method provided an overall optimum prediction for En15R steel.

In summary, the comparison between experimental results and theoretical predictions from the two life prediction methods reveals that the long-standing problem of multiaxial random fatigue can now be tackled with reasonable confidence. The two methodologies developed so far provide fair working estimates of fatigue endurance. Future work is, however, needed to examine the accuracy and efficiency of these two methods in dealing with real engineering components under service loading.

5 Conclusions

Two fatigue life prediction methods for multiaxial random loading are examined and comparison between predictions and experimental results made, from which the following conclusions can be drawn.

(1) Bannantine and Socie's method and Wang and Brown's method predict fatigue lifetime for proportional variable loading, with predictions falling within a factor of 1.5 on endurance.
(2) In the case of nonproportional variable loading, damage summations from Wang and Brown's method lie between 0.55 and 1.5, compared to those from Bannantine and Socie's method between 0.22 to 0.7.
(3) For general multiaxial random loading, Wang and Brown's method appeared to be a better choice than that by Bannantine and Socie, in terms of accuracy and computational efficiency.

Acknowledgements

The authors thank the sponsors of BRITE/EURAM programme BR/EU 3051, contract No. 0099, for financial support for the project.

References

(1) MATSUISHI, M. and ENDO, T. (1968) Fatigue of metals subjected to varying stress, presented to *Japan Society of Mechancial Engineers*, Fukuoka, Japan, March 1968.
(2) BURNS, A. (1956) Fatigue loading in flight: loads in the tailplane and fin of a Varsity, *Aeronautical Research Council Technical Report, C. P. 256*, London.
(3) DOWLING, N. E. (1972) Fatigue failure predictions for complicated stress-strain histories, *Journal of Materials*, **7**, pp. 71–87.
(4) OKAMURA, H. and SAKAI, S. (1979) Cumulative fatigue damage under random loads, *Fatigue of Engineering Materials and Structures*, **1**, pp. 409–419.
(5) DOWNING, S. D. and SOCIE, D. F. (1982) Simple Rainflow counting algorithms, *Int. J. of Fatigue*, **4**, pp. 31–40.
(6) BROWN, M. W. and MILLER, K. J. (1982) Two decades of progress in the assessment of multiaxial low-cycle fatigue life, *Low-Cycle Fatigue and Life Prediction*, ASTM Special Technical Publication 770 (editors C. Amzallag, N. B. Leis and P. Rabbe), American Society for Testing and Materials, Philadelphia, pp. 482–499.
(7) BANNANTINE, J. A. and SOCIE, D. F. (1991) A variable amplitude multiaxial fatigue life prediction method, *Fatigue under Biaxial and Multiaxial Loading*, ESIS Publication No. 10 (editors K. Kussmaul, D. McDiarmid and D. Socie), Mechanical Engineering Publications London, pp. 35–51.

(8) BANNANTINE, J. A. and SOCIE, D. F. (1992) Multiaxial fatigue life estimation techniques. *Advances in Fatigue Lifetime Predictive Techniques, ASTM STP 1122* (editors M. Mitchell and R. Sandgraf), American Society for Testing and Materials, Philadelphia.
(9) BROWN, M. W. and MILLER, K. J. (1978) A theory for fatigue failure under multiaxial stress strain conditions, *Proc. Instn. Mech. Engrs.* **187**, pp. 745–755.
(10) WANG, C. H. and BROWN, M. W. (1995) A cycle counting method for multiaxial random fatigue, Accepted for publication in *Fatigue and Fracture of Engineering Materials and Structures.*
(11) WANG, C. H. and BROWN, M. W. (1993) Inelastic deformation and fatigue under complex loading, *Trans. Twelfth Int. Conf. Structural Mechanics in Reactor Technology* (Stuttgart), Elsevier Science Publishers, Amsterdam, L, pp. 159–170.
(12) MINER, M. A. (1945) Cumulative damage in fatigue. J. of Appl. Mechanics, **12**, pp. A159–A164.
(13) WANG, C. H. and BROWN, M. W. (1993) A path-independent parameter for fatigue under proportional and nonproportional loading, *Fatigue and Fracture of Engineering Materials and Structures*, **16**, pp. 1285–1298.
(14) WANG, C. H. and BROWN, M. W. (1993) A study of deformation behaviour under multiaxial loading, European Journal of Mechanics, A/Solids, **13**, (2), pp. 175–188.
(15) WANG, C. H. and BROWN, M. W. (1991) Test results of En15R under biaxial loading. Departmental Report No. 125, Dept. of Mechanical and Process Engineering, The University of Sheffield.
(16) BROWN, M. W. and MILLER, K. J. (1985) Mode I fatigue crack growth under biaxial stress at room and elevated temperature, *Multiaxial Fatigue*, ASTM Special Technical Publication 853 (editors K. J. Miller and M. W. Brown), American Society for Testing and Materials, Philadelphia, pp. 135–152.
(17) WANG, C. H. (1990) The behaviour of short fatigue cracks under mean stress, Ph.D thesis, The University of Sheffield, U.K.
(18) BALOCH, R. A. and BROWN, M. W. (1993) Crack closure analysis for the threshold of fatigue crack growth under mixed mode I/II loading, *Mixed-Mode Fatigue and Fracture*, ESIS Publication No. 14 (editors H. P. Rossmanith and K. J. Miller), Mechanical Engineering Publications, London, pp. 125–137.
(19) BROWN, M. W., MILLER, K. J. and LIU, H. W. (1983) Multiaxial cumulative damage in low cycle fatigue, *Proc. ICF Int. Symp. on Fracture Mechanisms* (Beijing), Science Press, Beijing, pp. 629–634.
(20) IBRAHIM, M. F. E. (1981) Early damage accumulation in metál fatigue, Ph.D thesis, The University of Sheffield.
(21) ZHANG, Z. (1991) Short fatigue crack behaviour under different loading systems, Ph.D thesis, The University of Sheffield.
(22) MILLER, K. J. (1991) Metal fatigue – past, current and future, *Proc. Instn Mech. Engrs.* **205**, pp. 291–304.
(23) WEISS, J. and PINEAU, A. (1993) Continuous and sequential multiaxial low-cycle fatigue damage in 316 stainless steel, *Advances in Multiaxial Fatigue*, ASTM Special Technical Publication 1191 (editors D. L. McDowell and R. Ellis), American Society for Testing and Materials, Philadelphia, pp. 183–203.